NEAR-BOTTOM CURRENT MEASURED BY
ACOUSTIC SENSORS

K.A. Selanger[†] and T. Carstens[†],
River and Harbour Laboratory, Trondheim, Norway.

ABSTRACT

A vertical current profile has been measured with three
acoustic meters 60 cm, 100 cm and 200 cm from the sea bottom.
The depth at the measuring site was 84 metres. The profile
is found to depend on the time   scale of the water particle
motion. An Ekman-like turning of the current is also
observed, and the thickness of friction layers is estimated.
Comparison of the current data with wave measurements
indicates that the vertical transfer of surface wave energy
is 30-50 per cent less than first order wave theory
prescribes.

INTRODUCTION

To extrapolate a current profile through the bottom friction
layer is often requested, but very difficult to do with
satisfying accuracy and reliability of the result. One
important reason is that there is still a great shortage of
field data to support theoretical works on this subject
(1,2) or to cover the wide variety of practical situations.
The present work is mainly intended to contribute with
results and experiences from profiling the near-bottom
current by acoustic sensors under natural conditions.

[†] Address: Klaebuvegen 153, N-7034 NTH-Trondheim, Norway.

ARRANGEMENT

The location of the station is illustrated in Fig. 1. The
bottom mooring was located at 84 m depth slightly off-shore
the south-west part of the Norwegian coastal zone. The
geographical position was N59°16' E05°04'. In this area
the bottom falls smoothly off at a ratio of about 1:100.
One kilometre to the west the slope increases towards the
Norwegian trough.

The mooring and the instrument setup is sketched in Fig. 2.
Three selfrecording acoustic current meters were mounted on
a tetrahedral framework. The measuring levels were $z=60$ cm,
100 cm and 200 cm. Each instrument measured the current
simultaneously in two orthogonal directions parallel to the
bottom. The power and logging unit also syncronized the
measurements of the three instruments.

In the top of the rig, 3 m above the sea bed, an Aanderaa
current meter of the integrating type measured absolute-
values of the current velocity and the direction of the
mooring. None of the instruments were able to rotate.

Wave data were logged from a Datawell Waverider buoy 12 km
west of the bottom mooring. This was a permanent wave
measuring station, but the bottom topography in that area
was too irregular to be suitable for the near-bottom current
measurements. Later measurements indicate that the wave
power spectrum may be reduced as much as 50 per cent
from the location of the waverider to the bottom mooring.
The periods of the waves, however, seem to be very similar
in the two positions.

Wind observations were made at the island Utsira, see Fig. 1.
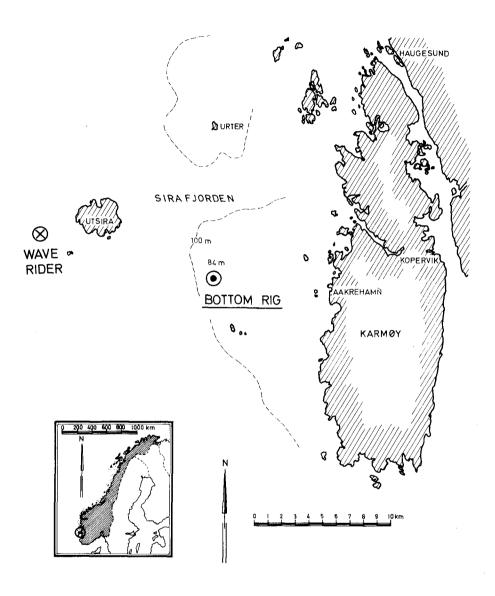These data were kindly supplied to us by the Norwegian
Meteorological Service.

Fig. 1. Location of the bottom mooring and the waverider
         buoy.

3.0 m —————
AANDERAA CURRENT METER
4
ACOUSTIC CURRENT METER
3
2.0 m —————

2
1.0 m —————
Z
0.6 m —————
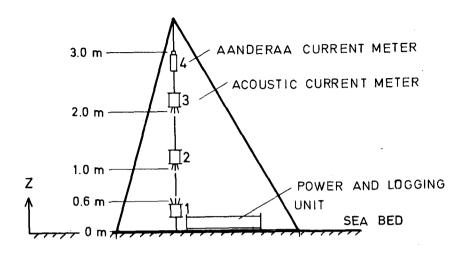POWER AND LOGGING
1
UNIT
SEA BED
0 m

Fig. 2.   The bottom mooring with instruments for profiling
          the current near the sea bed.

DATA SAMPLING AND OBSERVATIONS

The common logging unit of the acoustic sensors is
programmable, and to measure the water particle movements
on various time scales a broken-series sampling was chosen.
One time sequence consisted of 60 equal-spaced registrations
each third second. This gives 3 minutes long sampling
periods, which were repeated four times an hour. The field
experiment lasted 8 days, starting the 17th of March 1975
at 10 a.m. and ending the 25th of March at 12 a.m.

Nearly half a million data were stored on a magnetic tape,
which was about sixty per cent of the total storage capacity.
Of course, a selection of data for presentation here has to
be done. Fig. 3 shows the sequential average velocities
(u_{jk}, v_{jk}), while the details from the single sequence
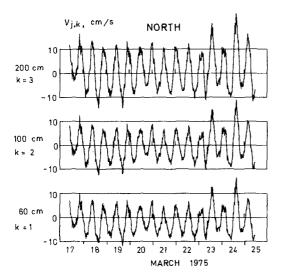$j=696$ are shown in Fig. 4.

At this point an account for the notation may be appropriate.
The current vector number i measured in sequence j by
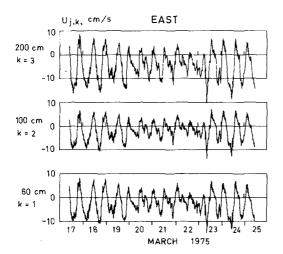instrument k is denoted

$$\vec{w}_{ijk} = (u_{ijk}, v_{ijk}) \tag{1}$$

In our case $i=1,2....,60$, $j=1,2....,775$ and $k=1,2$ and 3,
where k increases with the distance from the bottom. The
axis of each instrument were directed 97 degrees and 7
degrees from north, but in this presentation all data are
transformed into a uv reference system with positive values
of u and v directed to the east ($90°$) and north ($0°$),
respectively. When polar coordinates (w_{ijk}, ϕ_{ijk}) are used
the angle ϕ is identical with the compass direction. By
time averaging the indexing is left out. Further,
the large symbol W is reserved for absolute-value
averaging, while the small letter w is used in conjunction
with vector averaging, e.g. $w_{jk} = |\vec{w}_{jk}|$.

The wave height measurements are shown in Fig. 5. The upper
curve shows the maximum wave height, H_{max}, and the lower
one is the $H_{1/3}$ parameter. At the time when these measure-
ments were done the wave registration system had a low
regularity, which resulted in loss of valuable data both at
the start and the end of the registration period.

The presentation of data is closed by the wind observations
from Utsira, see Fig. 6. The diagram shows the average wind
velocity for the last 6 hours.

Fig. 3. Sequential mean values of the current velocity components, u_{jk} and v_{jk}, at the three levels z_k from the bottom. $z_1 = 60$ cm, $z_2 = 100$ cm and $z_3 = 200$ cm. A unit increment of the time index j corresponds to 15 minutes.
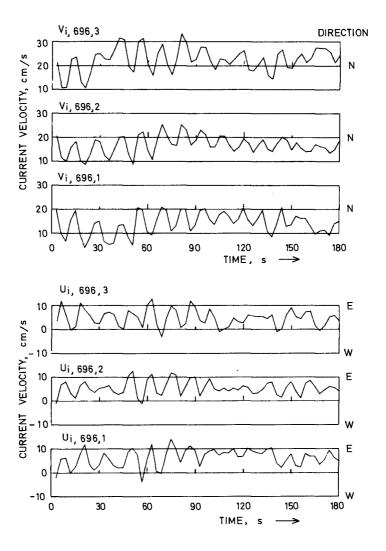
Fig. 4.   The acoustic current measurements of the sequence
j=696, $u_{i,696,k}$ and $v_{i,696,k}$.   k=1,2 and 3
indicate the distances 60 cm, 100 cm and 200 cm
from sea bed, respectively.   Sampling interval is
3 s.   The measurements were performed the 24th of
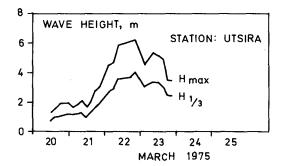March, 1975 at 4 p.m. at a station depth of 84 m.

Fig. 5.   The measured wave heights H_{max} and $H_{1/3}$.
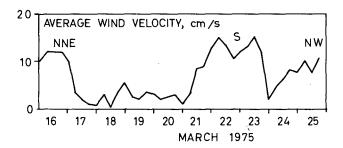
Fig. 6.   Wind observations.   The diagram shows the mean
          wind speed for the last six hours.

THE MEAN CURRENT AND THE EKMAN-LIKE TURNING

The analysis is started with the slowest varying motions of
the water.   These are illustrated by the progressive vector
diagrams in Fig. 7.   In fact these curves show the same data
u_{jk} and v_{jk} as Fig. 3, but this time the z-dependence of
the mean current vector is exposed more clearly.   The

characteristic tidal loops are also easily seen.

The average current speeds for the entire registration
period are $w_1 = 2.5$ cm/s, $w_2 = 1.8$ cm/s and $w_3 = 4.8$ cm/s. Hence,
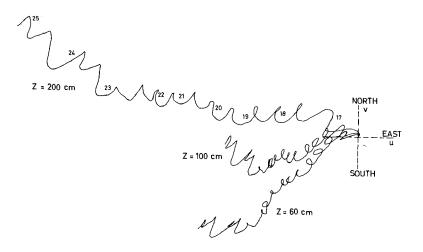w_2 is less than w_1, while w_3 is about twice of w_1.

Fig. 7.   Progressive vector diagrams of the bottom current.

During the five days long period from the 18th to the 22nd
of March the flow was reasonably steady towards the east and
the south. We therefore use this period for a closer inspec-
tion of the turning effect which is so clearly demonstrated
in this figure. The mean velocity for these days is listed
in Table 1 both on vector component form and as polar
coordinates. The vectors are drawn with solid lines in
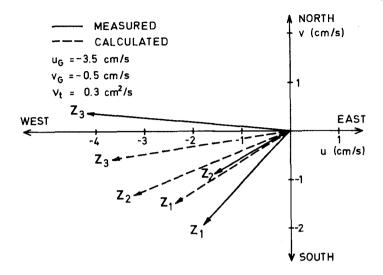Fig. 8.

Fig. 8.   Comparison of the mean velocity measured between
          the 18th and the 22nd of March with current values
          calculated from Ekman's theory.

According to Ekman's theory the Coriolis force causes a
turning of the current to the left as the distance from
the bottom is reduced. The differential equations are well
known and shall not be repeated here. Suggesting a
geostrophic current $w_G = (u_G{}^2 + v_G{}^2)^{\frac{1}{2}}$ for large values of
z and a no-slip condition at the bottom the turning of the
current is described by the integrated equations

$$u = u_G - w_G e^{-\frac{\pi}{D} z} \cos(\frac{\pi}{D} z + \beta) \tag{2a}$$

$$v = v_G + w_G e^{-\frac{\pi}{D} z} \sin(\frac{\pi}{D} z + \beta) \tag{2b}$$

where $D = \pi \left(\dfrac{2\,\nu_t}{f}\right)^{\frac{1}{2}}$ and $\beta = \mathrm{arctg}\left(-\dfrac{u_G}{v_G}\right)$.   D   is the

thickness of the frictional layer, ν_t is the eddy viscosity
and   f   is the Coriolis parameter.   For   z > D   the current
practically attains the constant velocity (u_G, v_G).   It is
also underlined that eq. (2) is based upon the assumption
that ν_t is independent of   z.

By systematic variation of the parameters u_G, v_G and ν_t
a best fit of eq. (2) to the measured current values in
Table 1 has been found. The parameter values, the friction
layer thickness   D   and the theoretical values of the current
speed $\vec{w}(z)$ are listed in Table 2. In addition the cal-
culated current vectors are drawn by dashed lines in Fig. 8
to visualize the comparison of experiment and theory. A
linear z-dependence of the eddy viscosity ν_t did not
improve the agreement between the theory and the field
data.

THE LONG-PERIODIC COMPONENTS OF THE CURRENT

The power density spectra in Fig. 9 show the long-periodic
harmonic components of the current. Note that the peak on
the frequency f_{15} is broken to blow up the other components.
No blocking or filtering has been applied. The power density
e_n is equal to

$$e_n = \frac{a_n{}^2 + b_n{}^2}{2\,\Delta f} , \quad n = 1,2,\ldots,30 \qquad\qquad (3)$$

where a_n and b_n are the amplitudes of the cosine- and sine
fourier coefficients, respectively, and Δf is the spectral

z (cm)	u (cm/s)	v (cm/s)	w (cm/s)	ψ
200	- 4.2	0.4	4.2	275°
100	- 1.6	- 0.9	1.8	241°
60	- 1.8	- 0.9	2.7	223°

Table 1.   The mean current vectors for the periode from the
           18th to the 22nd of March.

z (cm)	u (cm/s)	v (cm/s)	w (cm/s)	ψ
200	- 3.7	- 0.6	3.7	261°
100	- 3.3	- 1.3	3.5	248°
60	- 2.4	- 1.5	2.8	238°

$u_G = - 3.5$ cm/s, $v_G = - 0.5$ cm/s, $\nu_t = 0.3$ cm^2/s,
$D = 2.2$ m.

Table 2.   Theoretical values of the near-bottom current
           as calculated from eq. (2).   The parameters
           u_G, v_G and ν_t are adjusted to obtain as good
           agreement between measurements and theory as
           possible, see Table 1 and Fig. 8.

resolution. In our case $\Delta f = 1/186$ hour^{-1} $= 0.0053763$
hour^{-1}. The total energy σ^2 of the spectra is shown in
each diagram.

The main peak on frequency f_{15} is readily identified as the
semidiurnial tide. Nearly 100 % (per cent) of the energy of
the tidal component M_2 (period 12.42 hours) is on f_{15}.   In
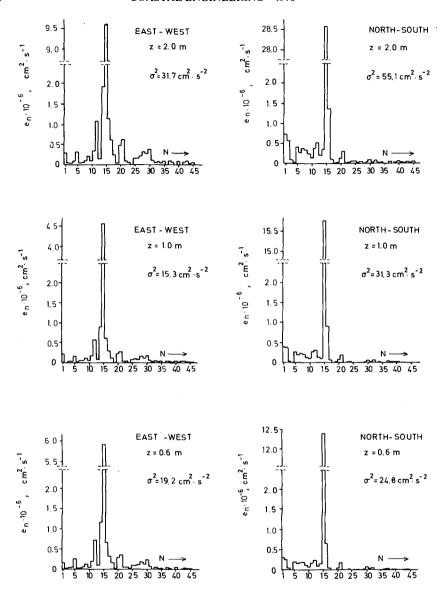addition N_2 (12.66 hours) and S_2 (12.00 hours) contributes

Fig. 9.   The longperiodic spectra computed from the
           data series (u_{jk}, v_{jk}) shown in Fig. 3.
           σ^2 is the standard deviation of the time
           series.

by 70 % and 40 %, respectively, of their energy to this
frequency. Due to the phase relationship the contribution
from S_2 is negative. The energy of f_{14} and f_{16} is mainly
due to S_2 and N_2. The first harmonic component of the main
peak, f_{30}, is very weak, but it seems to be significant.

The other spectral peaks are somewhat more difficult to
identify. The tidal component M_3 is expected at f_{22} and
f_{23} while the nearest top in the spectra is f_{20} and f_{21}.
The period of f_5 is 37.2 hours, which is characteristic of
the passage of a low pressure. Finally, we compare the
period of f_{12}, 15.50 hours, to the inertial period, 13.97
hours.

The attenuation of the longperiodic fluctuations due to the
bottom friction is somewhat different from what was observed
for the mean current. From 60 cm to 100 cm the energy
σ^2 increases very slightly, while the increase of σ^2 is
nearly 100 % between 100 cm and 200 cm from the bottom.
This corresponds to a difference in velocity of 30-40 %.

The main half axis of the rotational ellipses of the tidal
frequences at f_{15} are about 7 cm/s in the two lowest
levels z_1 and z_2, and 10 cm/s at z_3. There is no
evidence for a turning of the slow periodicities similar
to that observed for the mean current.

THE SHORT-PERIODIC FLUCTUATIONS

The variations of the current within each 3-minutes sequence
proved to be strongly connected to the windgenerated wave
condition on the sea surface, Figs. 5 and 6. Particularly
the wind from north the 24th and 25th of March induced
horizontal movements of the water particles like those shown
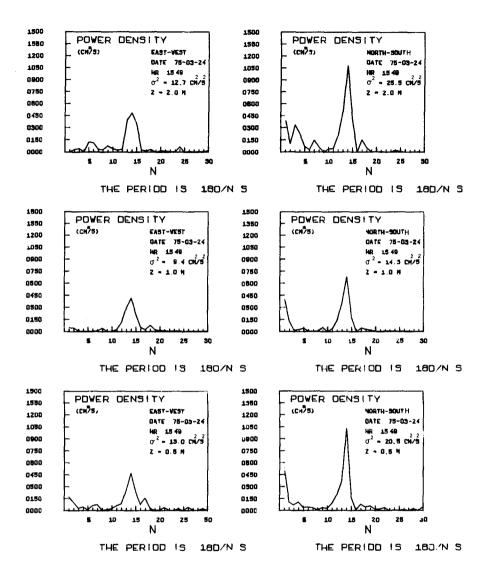in Fig. 4. Spectral estimates of these time series, see ·

Fig. 10.   Power spectra computed from the current measure-
ments $(u_{i,696,k}, v_{i,696,k})$.   The time series
are shown in Fig. 4.

Fig. 10, show a significant peak on typical wave periods
between 11 s and 16 s. Only a small part of the spectral
energy falls outside this top.
Except for a linear trend reduction the raw data series have
been applied for estimating these spectra.

These fast fluctuations seem to be less affected by the
bottom friction than the tidal current and the mean velocity.
There is a minimum of the peak power as well as the
spectral energy 100 cm from the bottom, but from 60 cm to
200 cm the increase of spectral energy is less than 20 %.
Similar studies of other time sequences confirm the result
that the friction layer thickness for movements on typical
wave frequences is less than 60 cm.
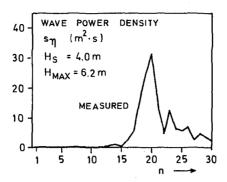

THE VERTICAL TRANSFER OF WAVE ENERGY

According to first order theory the spectral wave power s_η
is transferred vertically in the sea as

$$e(\delta) = T_\eta^2(\delta) \cdot s_\eta \qquad\qquad (4)$$

where δ is the depth and η indicates the wave profile.
The transfer function T_η is given by

$$T_\eta = \frac{2\pi f}{\text{sh } kd} \qquad\qquad (5)$$

where f is the frequency, $k = k(\delta,f)$ is the wave number
and d is the total depth. Having measured s_η and a velo-
city spectrum $e(\delta)$ the transfer function T_η can be
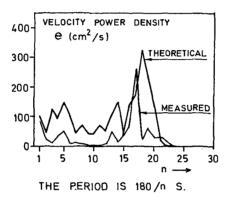tested directly.

Fig. 11. a) The surface wave spectrum $s_\eta(\delta=0\ m)$. H_s and
          H_{max} are the significant and the maximum wave
          height, respectively.
         b) The theoretical velocity spectrum $e(\delta=82\ m)$
          as computed by eqs. (4) and (5), and the
          measured spectrum $e(z=2\ m)$. The measurements
          were made the 22nd of March at 21 p.m., 1975.

Since the wave measurements stopped by accident too early,
the sequence of data shown in Fig. 4 cannot be used for
this purpose. Instead, the wave spectrum measured the 22nd
of March at 21 p.m. is used, see Fig. 11 a. The theoretical

spectrum computed by eqs. (4) and (5) is shown in the
diagram below, Fig. 11 b, together with the power density
measured simultaneously 200 cm from the bottom. Hence, the
parameters $d = 84$ m and $\delta = 82$ m. The power density of
both the u and v direction are included in the current
velocity spectrum.

The two spectra in Fig. 11 b indeed show a similar shape in
several details. However, there seems to be a greater
attenuation of the high frequency flange of the central peak
than the theory prescribes. The opposite flange fits quite
well at periods between 10 s and 12 s.

The energy of the wave-like motion close to the bottom is
found to be about 50 % less than expected from linear wave
theory applied to a measured wave spectrum. Some proposals
for explaining this discrepancy are discussed in the next
chapter.

DISCUSSION AND CONCLUSIONS

The acoustic current measurements have revealed how the
profile in the bottom friction layer depends on the
characteristic time of the water movement. After having
smoothed out the semidiurnal tide from the time series, a
mean current remains which increases by 100 % from $z_1 =$
60 cm to $z_3 = 200$ cm above sea bed.

The amplitude of the dominating tidal current increases by
40 % or so, while the oscillations on typical wave
frequences remains nearly constant over the same vertical
range. Therefore, one may conclude that the thickness of the
bottom friction layer is less than 60 cm for wind-generated
wave motions.

A current profile including the result from the Aanderaa
current meter has been drawn in Fig. 12. Since the Aanderaa
instrument did not rotate it only recorded mean values of
the absolute current speed, an operation which has been done
mathematically for the acoustic data. The registrations made
by the two different types of instruments seem to agree quite
well. As shown by a dashed line in Fig. 12 the logarithmic
function

$$W = \frac{W_*}{\kappa} \ln \frac{z + z_0}{z_0} \tag{6}$$

has been fitted to the data points. In eq. (6) W_* is
the frictional velocity, $\kappa = 0.4$ is von Karmans constant
and z_0 is the roughness parameter. Eq.(6) describes the
observations reasonably well with the parameters $W_* = 1.8$
cm/s and $z_0 = 23$ cm. This value of z_0 is high and
characterizes a hydrodynamically rough bottom. However,
when interpreting such a current profile, one should have in
mind how the friction layer thickness has been shown to
depend on the period of the motion.

An Ekman-like turning of the mean current has been demon-
strated, see Fig. 7. In Fig. 8 the experimental result is
compared with the idealized Ekman theory where the parameter
values $\nu_t = 0.3$ cm/s^2, $u_G = -3.5$ cm/s and $v_G = -0.5$ cm/s are
used. The Ekman friction layer is estimated to be 2-3 m
thick. The observed turning is greater than the theory pre-
scribes, and the measured average current for $z = 100$ cm
has only half the expected value. This disagreement may be
due to a) topographical effects, b) calibration errors,
or c) that ν_t depends on z and t and also is influenced
by the tide. It should also be pointed out that since the
mean current is weak small inaccuracies may result in large
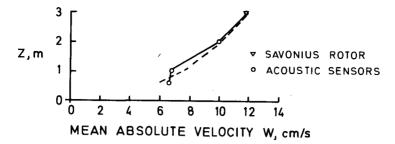relative errors.

Fig. 12.   The current profile including the registrations by
          the Aanderaa meter. The broken line shows a loga-
          rithmic profile, eq. (6), with W_* = 1.8 cm/s and
          z_0 = 23 cm.

Later experiments indicate that stratification effects are
negligible. The boundary condition (u_G, v_G) was not measured.

A velocity component closely related to the wind-generated
surface waves is also observed. The intensity of these fast
fluctuations is about 50 % less than expected from linear
wave theory. This trend, suggesting a weaker wave action
near the bottom than classical theory predicts, is in accord
with earlier results obtained with pressure sensors,
summarized by Silvester, (3).   However, the attenuation we
have observed seems to be somewhat stronger, and this
discrepancy may be caused by the different location of the
Waverider buoy and the bottom mooring. The influence of the
bottom friction on these fast fluctuations is found to be
insignificant beyond z = 60 cm.

REFERENCES

[1] : Weatherly, G.L.: A Study of the Bottom Boundary Layer of the
            Florida Current. J. Phys. Osc. Vol. 2. pp 54-72. Jan. 1972

[2] : Knight, D.W.: Review of Oscillatory Boundary Layer Flow. J. Hydr.
            Div. ASCE.Vol. 104 No HY6. pp 839-855. June 1978.

[3] : Silvester, R.: Coastal Engineering I. Elsevier Publ. Comp.
            1974, pp 275-290.